Downregulation of Lipid Phosphate Phosphatase 3 correlates with Tumor-Infiltrating Immune Cells in Oral Cancer

Supriya Vishwakarma
All India Institute of Medical Sciences
Deepti Joshi
AIIMS: All India Institute of Medical Sciences
Ritu Pandey
AIIMS: All India Institute of Medical Sciences
Saikat Das
AIIMS: All India Institute of Medical Sciences
Sramana Mukhopadhyay
AIIMS: All India Institute of Medical Sciences
Renu Singh
JNCHRC: Jawaharlal Nehru Cancer Hospital and Research Centre
Ritu Singhal
JNCHRC: Jawaharlal Nehru Cancer Hospital and Research Centre
Neelkamal Kapoor
AIIMS: All India Institute of Medical Sciences
Ashok Kumar (ashok.biochemistry@aiimsbhopal.edu.in)
All India Institute of Medical Science - Bhopal https://orcid.org/0000-0001-7208-2947

Research Article

Keywords: Head and Neck Cancer, oral squamous cell carcinoma, Sphingosine-1-Phosphate, Sphingosine Kinase 1, Sphingosine Kinase 2, SGPP1, Lipid Phosphate Phosphatase 3

Posted Date: November 19th, 2021

DOI: https://doi.org/10.21203/rs.3.rs-1043910/v1

Version of Record: A version of this preprint was published at Cureus on March 27th, 2022. See the published version at https://doi.org/10.7759/cureus.23553.

Title: Downregulation of Lipid Phosphate Phosphatase 3 correlates with Tumor-Infiltrating Immune Cells in Oral Cancer

Short Running Title: Downregulation of LPP3 in OSCC

Authors: Supriya Vishwakarma[1], Deepti Joshi[2], Ritu Pandey[1], Saikat Das[3], Sramana Mukhopadhyay[2], Renu Singh[3], Ritu Singhal[4], Neelkamal Kapoor[2], Ashok Kumar[1]*

Affiliations: [1]Department of Biochemistry, [2]Department of Pathology and Laboratory Medicine, [3]Department of Radiotherapy, All India Institute of Medical Sciences (AIIMS) Bhopal, Saket Nagar, Bhopal, 462 020 India

[4]Jawaharlal Nehru Cancer Hospital and Research Center, Idgah Hills, Bhopal, India

Address for Correspondence

*Dr. Ashok Kumar, Associate Professor, Department of Biochemistry, All India Institute of Medical Sciences (AIIMS) Bhopal, Saket Nagar, Bhopal, 462 020 India

Phone: +91-755-2672347

E-mail: ashok.biochemistry@aiimsbhopal.edu.in

ORCID ID: 000-0001-7208-2947

Abstract

Purpose: Sphingosine-1-phosphate (S1P), a potent oncogenic lipid. Intracellular levels of S1P are tightly regulated by eight S1P metabolizing enzymes. S1P is synthesized by phosphorylation of sphingosine which is catalyzed by two sphingosine kinases (SphK1 and SphK2). Five lipid phosphatases (two S1P phosphatases and three lipid phosphate phosphatases) reversibly convert S1P back to sphingosine. S1P is ultimately irreversibly degraded by S1P lyase. The role of sphingosine-1-phosphate (S1P) metabolizing enzymes in oral squamous cell carcinoma (OSCC) has not been fully studied.

Methods: In the current study, we have determined the protein expression of four S1P metabolizing enzymes, namely sphingosine Kinase (SphK) -1, SphK2, S1P phosphatase 1 (SGPP1), and lipid phosphate phosphatase 3 (LPP3) by immunohistochemistry (IHC) and western botting in tumor tissues of 46 OSCC patients and normal oral mucosa (N = 6). Further, we determined the associations of expression of S1P metabolizing enzymes with clinicopathological features of OSCC patients.

Results: SphK2 and LPP3 exhibit low IRS in OSCC tumors. Importantly, expression of SphK2 and LPP3 was downregulated in malignant cells compared to non-malignant mucosa. Further, LPP3 expression negatively correlated with TNM staging of patients ($\rho = -0.307$, $p = 0.043$). Importantly, TCGA analysis revealed that LPP3 expression was positively correlated with infiltration of B cells, neutrophils, macrophages, and dendritic cells in the HNSCC tumors.

Conclusion: In conclusion, our data show that expression of SphK2 and LPP3 is decreased in OSCC tumors compared to normal mucosa. Thus, LPP3 could represent a potential prognostic marker and therapeutic target for OSCC.

Key Words: Head and Neck Cancer, oral squamous cell carcinoma, Sphingosine-1-Phosphate, Sphingosine Kinase 1, Sphingosine Kinase 2, SGPP1, Lipid Phosphate Phosphatase 3

Introduction:

Head and neck cancer (HNC) is the sixth most common cancer globally (Bray et al. 2018). As per GLOBOCON 2018 data, the age-standardized rate per 100,000 for cancer of the lip and oral cavity in males is twice in developing countries than in developed countries (Bray et al. 2018). The majority of the oral cavity, oropharyngeal, hypopharyngeal, and laryngeal cancers are squamous cell carcinoma (SCC) in histology. Squamous cell cancer of the lip and oral cavity are referred to as oral squamous cell carcinoma (OSCC), which is the most common cancer in Indian men and accounts for one-sixth of all cancers (Mallath et al. 2014). The global incidence of OSCC is more than 350,000 (Bray et al. 2018), out of which one-fourth of the cases (75,000) is contributed by the Indian sub-continent (Mallath et al. 2014). Rapid advances in diagnosis, availability of prognostic markers, and early management protocols have not increased the five-year survival rate.

Management of OSCC includes surgery, chemotherapy, radiotherapy, and combination therapy depending on site, age, and tumor-node-metastasis (TNM) staging. Conventional therapies are nonselective and often remove normal tissues in the complex orofacial region (Jain et al. 2019). Molecularly-targeted therapies offer new treatment options even for patients who are unable to tolerate chemotherapy or radiation therapy. Though, epidermal growth factor receptor antibody (cetuximab) offers clinical gain; however, intrinsic resistance, and the development of acquired resistance to cetuximab are well-recognized phenomena in OSCC. Therefore, identifying novel oncogenic pathways in OSCC could lead to the development of targeted therapy combinations and overcome drug resistance.

Sphingosine-1-phosphate (S1P), a potent sphingolipid metabolite, mediates its actions by binding to its cognate G-protein coupled receptors, termed S1P receptors (Kumar and Saba 2018). S1P has diverse pleiotropic biological functions, including lymphocyte trafficking, vascular angiogenesis, and muscle regeneration (Kumar and Saba 2018). S1P signaling regulates several processes integral to carcinogenesis, including inflammation, cancer initiation, progression, invasion, metastasis, and drug and radiation resistance (Kumar and Saba 2018; Nagahashi et al. 2018; Ogretmen 2018). However, the role of S1P signaling in oral carcinogenesis is not fully understood.

Eight metabolic enzymes tightly regulate intracellular S1P levels. S1P is synthesized intracellularly by two sphingosine kinases (SphKs), namely SphK1 and SphK2. Both the isoforms catalyze the phosphorylation of sphingosine to form S1P (Hatoum et al. 2017). Further, the catabolism of S1P is regulated by six enzymes. Out of six S1P catabolizing enzymes, two are S1P phosphatases viz. SGPP1 and SGPP2 that dephosphorylate S1P back to

sphingosine (Le Stunff et al. 2002; Ogawa et al. 2003; Ogretmen 2018). In addition, broad-specificity lipid phosphate phosphatases (LPPs) -1, -2, and 3, can also dephosphorylate S1P (Brindley and Pilquil 2009; Benesch et al. 2016). Importantly, S1P lyase irreversibly degrades S1P into a hexadecenal and ethanolamine phosphate (Kumar and Saba 2018).

SphK1 is linked with pro-survival and cell maintenance functions (Hatoum et al. 2017); however, its second isoform, SphK2, has been shown to perform dual tasks, i.e., a protective role in cell maintenance as well as its pro-apoptotic functions (Hatoum et al. 2017). SphK1 promotes tumor progression, invasion, metastasis, and chemoresistance and is a well-established oncogene (Hatoum et al. 2017). SphK1 is abundantly expressed in various types of cancers, including OSCC, and a marker for poor prognosis (Hatoum et al. 2017). Low increase in SphK2 levels (2.5 fold), compared to the levels in corresponding normal tissue, could potentially promote cell proliferation and neoplastic transformation. In contrast, high levels of SphK2 are associated with pro-apoptotic signaling, predicted to be through the unique BH3 pro-apoptotic domain that dominates over the proliferative SphK2/S1P response (Neubauer et al. 2016).

Except for SphK1, the role of S1P metabolizing enzymes in OSCC has not been fully understood. Earlier, we reported that in approximately two-thirds of OSCC patients studied, mRNA expression of SphK2 and LPP3 was significantly downregulated in tumor tissues, compared with the same patient's adjacent normal tissue (Vishwakarma et al. 2017). Since no information is available regarding immunohistochemical localization of SphK2, SGPP1, and LPP3 in OSCC, thus, in the present study, we have analyzed the expression of SphK1, SphK2, SGPP1, and LPP3 in tumor tissues from OSCC patients and benign oral mucosa by immunohistochemistry (IHC).

The tumor microenvironment (TME) of HNSCCs consists of many different subsets of cells, including cells of the immune system that infiltrate the tumors (Chen et al. 2020). Emerging evidence from recent studies suggests that tumor-infiltrating immune cells (TIICs) play an essential role in immunogenic cytotoxicity and tumor response to establish immune tolerance (Lei et al. 2016; Chen et al. 2020). TIICs, especially tumor-infiltrating lymphocytes (TILs), are critical prognostic features of HNSCC tumors. The presence of effector immune cells in the tumor microenvironment is associated with a better clinical response to chemo-radiation (Hladíková et al. 2019; Chen et al. 2020). S1P signaling has emerged as a central regulator of the trafficking of immune cells, including lymphocytes,

natural killer (NK) cells, neutrophils, dendritic cells (DCs), and macrophages (Ogretmen 2017). However, the role of S1P metabolizing enzymes in the regulation of TIICs in HNSCC has not been elucidated.

Further, we have determined the association of expression of S1P metabolizing enzymes with clinicopathological attributes of OSCC patients. Here, we demonstrated that the expression of SphK2 and LPP3 was downregulated in OSCC tumors compared to non-malignant mucosa. Further, LPP3 expression negatively correlated with TNM staging of patients (ρ=0.-307, p=0.043). In a multivariate analysis, we found that expression of LPP3 is an independent predictor of perinodal extension (β=-0.440, p=0.009), lympho-vascular invasion (β=-0.614, p<0.001), lymph node ratio (β=0.336, p=0.039) and TNM staging (β=-0.364, p=0.030). In the TCGA analysis, LPP3 expression correlated with the infiltration levels of B cells, Tregs, neutrophils, macrophages, and DCs in HNSC tumors.

Materials and Methods

Subjects and Tissue collection

Forty-six patients with OSCC (ICD-10: C00-08) over the age of 18 years, who had not undergone radiotherapy and chemotherapy were enrolled in the study at Jawaharlal Nehru Cancer Hospital & Research Centre, Bhopal. In addition, six subjects with non-dysplastic oral mucosa were also included in the study. Informed consent was obtained from all the participants. Data on the initial diagnosis and clinical history of patients were recorded. The above project was approved by the Institutional Human Ethics Committee, AIIMS Bhopal.

Western Blotting

Tumor and adjacent normal tissues (at least 1 cm away from tumor margin) were collected in microcentrifuge tubes and flash frozen in liquid nitrogen immediately after surgical resection. Approximately, 50 mg of tissue was homogenized in a lysis buffer containing 150 mM NaCl, 1 mM MgCl2, 1 mM NaF, protease inhibitor cocktail and 1% triton-X 100. Total protein was quantitated using Bradford's reagent (Bio-Rad Laboratories). Forty microgram protein was separated on 10% sodium-dodecylsulphate polyacrylamide gel electrophoresis (SDS-PAGE). Proteins were electrotransferred to nitrocellulose membrane. Non-specific sites were blocked by 10% non-fat milk in Tris-buffer saline containing 0.05% Tween-20. Membranes were incubated with primary antibodies, human SphK2 (Cat#

SAB1300017) (Sigma-Aldrich, St. Louis, MO), human SGPP1 (Biorbyt, Cambridge, UK), human LPP3 (Cat# HPA028892, Sigma) and beta actin (Sigma-Aldrich). After washing, membranes were incubated with horse-radish peroxidase conjugated secondary antibody. Immune complexes were recognized with enhanced chemiluminescence substrate (ThermoFisher Scientific). Signals were captured with a Chemidoc (Syngene). Intensity of bands were quantitated with Image J software (NIH, Bethesda).

IHC

All Immunohistochemical analyses were carried out using the Vectastain Universal Elite ABC Kit. Tissue sections (4-5 micron) were mounted on glass slides using 3-Aminopropylenetriethoxysilane (APES) solution (1:20 in methanol) and deparaffinized in a hot-air oven for 10 minutes. Further deparaffinization was done with xylene and rehydrated with graded alcohol. Endogenous peroxidase activity was blocked with 3% hydrogen peroxide in methanol for 20 min, followed by PBS wash thrice. Antigen retrieval was done by immersing slides in 10 mM Sodium Citrate buffer (pH 6.0) and placed in a microwave for 20 min to enhance antigen exposure. Then, blocking was done with normal goat serum for 1 hour, followed by incubation with the primary antibody at 1:100 dilution in blocking buffer (normal goat serum) overnight at 4 °C. Rabbit polyclonal antibodies against human SphK1 (Cell Signaling Technology, Danvers, MA), human SphK2 (Cat# SAB1300017) (Sigma-Aldrich, St. Louis, MO), human SGPP1 (Biorbyt, Cambridge, UK), and human LPP3 (Cat# HPA028892, Sigma) were used as the primary antibodies. Immunostaining was developed using the Vectastain ABC reagents (Vector Laboratories, Burlingame, CA, USA), according to biotinylated immune-peroxidase technique followed by 3, 3′-diaminobenzidine (DAB substrate) staining. Tissue sections were counterstained with hematoxylin.

Assessment of immunohistochemical staining

Immunoreactivity for SphK1, SphK2, SGPP1, and LPP3 was semi-quantitatively estimated by combining intensity and percentage of positive tumor cells under the microscope. The immunostaining results were optimized and judged by two independent pathologists according to the following standards. Atleast five fields were examined in each section. Based on the all the field view, the immunoreactivity score was calculated for each slide. The staining intensity

was scored as follows: 0 (negative staining), 1 (mild staining), 2 (moderate staining), and 3 (strong staining). The percentage of stained cells was classified as follows: 0 (<10%), 1 (10-50%), 2 (51%–80%), and 3 (>81%). The final immunoreactivity score (IRS) for each protein, ranging from 0 to 9, was obtained by multiplying the percentage of positive cells and the intensity score. Patients with a final IRS score were classified as low (1-4) and high (≥5). Tumor-infiltrating immune cells (TIICs) were counted in the high-power field of hematoxylin & eosin-stained sections of OSCC tumors. Immunostaining were performed with consecutive sections with all antibodies Results were interpretated by atleast two pathologists.

Association of mRNA expression of S1P metabolizing genes and immune cells

Tumor Immune Estimation Resource (TIMER) is a web server for the comprehensive analysis of tumor-infiltrating immune cells (Li et al. 2017). The group has launched the updated and enhanced version of the web-server, TIMER2.0, which can be used to systematically analyze immune infiltration across diverse cancer types (Li et al. 2020). TIMER2.0 (http://timer.cistrome.org/) provides a more robust estimation of immune infiltration levels for TCGA or user-provided tumor profiles using six algorithms (Li et al. 2020). Association between mRNA expression of S1P metabolizing enzymes and TIICs (B cells, CD4+ T cells, CD8+ T cells, regulatory T cells (Tregs), neutrophils, macrophages, DC and NK cells) was analyzed by the 'Immune' module of TIMER 2.0, where gene expression profile from HPV negative (n=422) and HPV positive (N =98) and HNSCC patients (N=522). Gene_DE module of TIMER 2.0 was used to study the differential expression between tumor and adjacent normal tissues for PPAP2B across all TCGA tumors.

Knockdown of LPP3 using Lentiviral shRNA

The human cervical cancer cell line, Ca Ski (ATCC-CRL-1550™) was obtained from American Type Culture Collection. The cell line was maintained in DMEM-F12 (Gibco, Grand Island, New York, USA), supplemented with 10% fetal bovine serum (Gibco), 100 units/ml of penicillin and streptomycin (Gibco), and 0.4 µg/ml hydrocortisone (MP Biomedicals India Pvt Ltd, Mumbai, India). The cell line was cultured in a humidified atmosphere at 37°C and 5% CO2. To knockdown the expression of *PPAP2B* gene coding for LPP3, 0.3 million Ca Ski cells were seeded in 6 well plate; upon reaching 60-70% confluency, cells were transfected with 4 µg of shControl and pLKO.1-shPPAP2B

(TRC No. TRCN0000050457, Sigma, Saint Louis, USA) using Fugene (Promega, Wisconsin, US) at 1:2 ratio (DNA Plasmid: Fugene), after 60 hrs of incubation at 37 ° C and 5% CO2, cells were retrieved for western blot analysis.

Overexpression of LPP3 in Tongue Squamous Cell Carcinoma Cells

Human tongue squamous cell carcinoma cell line, SCC-9 cells were maintained in DMEM:F12 media supplemented with fetal bovine serum, antibiotics and 0.4 µg/ml hydrocortisone at 37°C with 5% CO2. To overexpress LPP3, 0.4 million SCC-9 were seeded in 6 well plate, upon reaching 60-70% confluency, cells were transfected with 2 µg of pEZY3-LPP3 or empty vector pEZY3 (a kind gift from Prof. David N Brindley, University of Alberta, Edmonton) using Fugene at 1:2 ratio (DNA Plasmid: Fugene), after 48 hrs of incubation, cells were harvested for western blot analysis.

Statistical analysis

Data was entered in SPSS software 21.0 (IBM, Armonk, New York). Descriptive analysis was done by SPSS software. Patient data, including age, gender, tobacco chewing, type of tobacco/betel nut consumed, alcohol consumption, site of tumor, history of smoking, tumor volume, TNM staging, lymph node ratio (LNR), lympho-vascular invasion (LVI) and perinodal extension (PNE) were entered into the database. The difference in the mean was determined by Student's t-test. To determine the association of IHC expression in OSCC of various S1P metabolizing enzymes, data from patients were categorized into two groups; low expression and high expression. The association of IRS with clinicopathological features was examined by Spearman's rank test. To determine clinicopathological attributes as an independent predictor of expression of S1P metabolizing enzymes or vice versa, multivariate linear regression analysis was performed.

Results

Patients Characteristics

The median age of the OSCC patients enrolled in the study was 46 years (25-75 years), and approximately two-thirds (67.40%) of subjects were male. More than half (58.7%) patients were younger than 50 years of age. Three-fourths of the subjects had a history of tobacco/betel nut chewing (78.30%). Approximately more than one-fourth of the subjects had a history of alcohol consumption or smoking (**Supplementary Table 1**). Buccal mucosa was the most common (50%) site for oral cancer in the subjects, followed by the tongue (26%) (**Supplementary Table 1**). More than three-fourth (78.2%) were presented in the advanced stages (stage III+IV) of OSCC (**Supplementary Table 1**); however, no distant metastasis was observed in our study. Histologically, most of the OSCC tumors (82.6%) were well-differentiated squamous cell carcinoma (WDSCC) (**Supplementary Table 1**).

Validation of antibodies

To validate the antibodies, immunoblotting was performed on four sets of tissue extracts (tumor and adjacent normal tissue) from OSCC patients. SphK2, LPP3, and SGPP1 detected a single prominent band in the gels (**Supplementary Figure S1A-E**). The molecular weight of mature LPP3 is 32 kDa, but LPP3 antibody used in our research paper detected a prominent band at ~57 kDa (**Supplementary Figure S1A**). On prolonged exposure of the LPP3 blot, two additional bands corresponding to ~32 kDa and ~37 kDa also appear in few samples (**Supplementary Figure S1B**). LPP3 is known to be heavily glycosylated, and similar bands have been detected by others (Waggoner et al. 1995) (Wary and Humtsoe 2005). Detection of a single prominent band by these antibodies establishes their specificity. To validate the specificity of LPP3, IHC was performed in lymph node, where LPP3 is responsible for maintaining low interstitial S1P levels (Simmons et al. 2019). As shown in **Supplementary Figure S2**, diffuse cytoplasmic positivity was observed in the lymphoid cells. Owing to the downregulation of LPP3 in tumor tissues from several cancer types (Tang and Brindley 2020), cancer cell lines also exhibit low expression of LPP3. We screened several cell lines to evaluate LPP3 expression. We found that Ca Ski, a cervical cancer cell line shows an appreciable level of LPP3

(**Supplementary Figure 3)**. Thus, to validate the specificity of the LPP3 antibody, *PPAP2B* gene was knocked down in Ca Ski cells using lentiviral vector. Transient transfection with a pLKO.1-shPPAP2B, decreased the expression of prominent LPP3 band to ~50 % compared to control shRNA transfected cells (**Supplementary Figure 3A**). Upon prolonged exposure, a decrease in the expression of a smaller band of ~37 kDa LPP3 protein was also noted in pLKO.1-shPPAP2B cells, compared to control shRNA (**Supplementary Figure 3A**, middle panel). To further validate the specificity of the LPP3 antibody, human tongue squamous carcinoma cells, SCC-9 cells were transiently transfected with a plasmid encoding for LPP3 or an empty vector. The cell lysate from LPP3 overexpressing cell line and vector control were subjected to western blotting with an anti-LPP3 antibody. SCC-9 cells transfected with vector control showed undetectable levels of LPP3 (**Supplementary Figure S3C)**, whereas LPP3-overexpressing cells showed a similar pattern as seen in the normal oral mucosa (**Supplementary Figure S1B and S3C**). Western blotting of LPP3-overexpressing SCC9 cells showed a major band at~57 kDa and three smaller bands. Two bands correspond to ~37 kDa and ~32 kDa, were also observed in LPP3-overexpressing cells; these bands were of similar size, as observed in the normal oral mucosa (**Supplementary Figure S1B and S3C**).

SphK1 is overexpressed in OSCC tumors

Our previous study has shown that SphK1 mRNA transcript is overexpressed in tumor tissues of OSCC patients compared to adjacent normal tissues from the same patient. To determine if it is consistent at the protein level, we performed IHC analysis on tumors from OSCC patients. Cytoplasmic positivity for SphK1 was observed in most tumor cases in malignant squamous epithelial cells (**Figure 1 A-B**). IRS score ranged from 2-9 in the OSCC cases with positive staining. All the cases included in the study were positive for SphK1. More than half (52.2%) showed high positivity in tumor cells (**Figure 1 C-D**), whereas low IRS for SphK1 was observed in 47.8% of patients. The mean IRS for SphK1 in all the cases was 4.78. Expression of SphK1 was higher in tumor cells compared to adjacent non-neoplastic cells (**Figure 1A**). Focal cytoplasmic positivity was also observed in the adjacent non-neoplastic epithelium in few cases. Amongst the non-epithelial tissues, cytoplasmic positivity was also noted in the stromal cells like inflammatory cells, skeletal muscle fibers, neural bundles, and blood vessels (**Figure 1D-F**).

SphK2 expression is downregulated in OSCC tumors

Strong cytoplasmic positivity for SphK2 was noted in normal mucosa (**Figure 2 A-D**). High immunoreactivity was observed in normal mucosa. On the other hand, IRS ranged from 2-6 (Mean IRS = 3.24) in all the OSCC cases except one sample, where the IRS was 9.0. Although immunoreactivity was noted in almost all the cases (96%); however, more than three-fourths (80.4%) of the cases showed low expression of SphK2. High immunoreactivity was noted in 17.4% of cases, and it was mostly seen in the adjacent non-malignant cells. Expression of SphK2 in adjacent non-malignant epithelium showed moderate to strong cytoplasmic positivity, whereas low expression was noted in tumor cells (**Figure 2 E-F**). The cytoplasmic activity was also recorded in skeletal muscle fibers and neurovascular bundle (**Figure 2 G-H**).

SGPP1 expressed at a low level in OSCC tumors

Cytoplasmic positivity for SGPP1 was observed in the majority of the cases. IRS score ranged from 1-6 (mean IRS = 3.8). Although immunoreactivity was noted in almost all (89%) the cases; however, approximately two-thirds (63%) of the cases showed low expression of SGPP1, whereas 26% cases showed high expression of SGPP1. Focal positivity was also noted in the adjacent non-neoplastic epithelium (**Figure 3**).

LPP3 expression is sharply downregulated in OSCC tumors

Strong cytoplasmic and membranous immunoreactivity was noted for LPP3 in the normal oral mucosa (**Figure 4A and B**). In OSCC, 17% of cases were negative for LPP3 immunoreactivity, 58.7% of cases showed low immunoreactivity, and only 24% of cases showed high expression. The mean IRS for LPP3 in OSCC tumors was 2.89. Even in the same tissue section from OSCC patients, adjacent non-malignant cells showed high immunoreactivity compared to tumor cells (**Figure 4A and B**). IRS was statistically lower in the tumor tissues compared to non-malignant tissues.

Expression of SphK2 and LPP3 is decreased in the tumor tissues than the adjacent normal tissue

To validate our findings, expression of SphK2, LPP3, and SGPP1 was analyzed by western blotting in four sets of tumor tissues and adjacent normal tissues from the same patients. As shown in **Figure 5A-G**, expression of LPP3 and SphK2 was decreased in three out of four samples (Figure 5A). Quantitative analysis showed a significant decrease in LPP3/beta-actin ratio in the tumors compared to the corresponding adjacent normal tissue (**Figure 5A-C**).

Association of IRS of S1P metabolizing genes with clinicopathological features

SphK1 is overexpressed and negatively correlates with poor survival of patients (Kato et al. 2018). However, the clinical significance of other S1P metabolizing enzymes in OSCC is not known. Association between S1P metabolizing enzyme expression (IRS) in tumors and clinicopathological features (age, gender, tobacco chewing, smoking status, alcohol consumption, tumor volume, tumor site, TNM staging, LNR, PNE, and LVI) was analyzed by Spearman's rank test. In the present study, the IRS of SphK2 negatively correlated with gender (ρ=-0.319, p=0.030). Female OSCC patients had lower IHC scores compared to males. IRS of SphK2 also negatively correlated with smoking status (ρ=0.-314, p=0.033).

IRS of SGPP1 positively correlated with LNR (ρ=0.313, p=0.040). OSCC patients with low SGPP1 IRS had low LNR (<0.1). Importantly, LPP3 expression negatively correlated with TNM staging of patients (ρ=0.-307, p=0.043) and LVI (ρ=-0.530, p<0.001). OSCC patients presented in the advanced stages (III+IV) of the disease had low IRS for LPP3.

Clinicopathological features as an independent predictor of expression of S1P metabolizing enzymes

To find out whether clinicopathological attributes (age, gender, tobacco chewing, smoking, alcohol consumption, tumor volume, TNM staging, PNE, LVI, and LNR) of OSCC patients could serve as an independent predictor of IRS in protein expression of S1P metabolizing genes, multivariate linear regression analysis was performed. Tumor size (Standardized coefficient β = 0-.562, p = 0.035), gender (Standardized coefficient β = -0.444, p = 0.040), and smoking status (Standardized coefficient β = -2.240, p<0.001) were found to be an independent negative predictor of SphK2

expression. LVI was found to be a strong negative predictor of LPP3 expression (standardized coefficient $\beta = -0.653$, $p = 0.002$).

S1P metabolizing gene expression as a predictor for clinicopathological features

To determine whether protein expression of S1P metabolizing enzymes in tumors could determine clinicopathological features (tumor volume, TNM staging, PNE, LNR, and LVI) of OSCC patients, multivariate linear regression analysis was done. The IRS of LPP3 in tumors was found to be an independent predictor of TNM staging (standardized coefficient $\beta = -0.364$, $p = 0.030$), PNE (Standardized coefficient $\beta = -0.440$, $p = 0.009$), LVI (standardized coefficient $\beta = -0.614$, $p<0.001$) and LNR (standardized coefficient $\beta = 0.336$, $p = 0.039$).

LPP3 expression correlates with infiltration of immune cells in HNSCC tumors

The role of the S1P metabolizing enzyme and S1P receptors in the regulation of infiltration of immune cells to the tumor stroma in HNSCC is not known. Correlation between TIICs and the IRS of S1P metabolizing enzymes was determined by Spearman's rank test. A trend of positive correlation ($\rho = 0.22$) was obtained between the number of TIICs in the OSCC tumors and IRS of LPP3, which did not reach statistical significance due to the low sample size.

To further analyze the association between the expression of S1P metabolizing genes and TIICs, TCGA data was analyzed by TIMER 2.0, a web-based server. In TIMER 2.0, correlation is determined by Spearman's rank test, and a heat map is generated based on positive, negative, or no significant correlation obtained from different algorithms (Li et al. 2020). As shown in **Figure 6A**, LPP3 showed moderate to a high positive correlation with the infiltration level of B cells, Tregs, neutrophils, M1 macrophages, and DC in HNSC tumors. The correlation was consistent in both the subtypes HPV negative and HPV positive HNSC tumors with different algorithms (**Figure 6A**), and representative plots are shown in **Figure 6B**. LPP3 did not show a consistent correlation with infiltration level of CD4+, CD8+ T cells, and NK cells. SphK2 expression consistent positive correlation with the infiltration level of B cells and Tregs, whereas SGPP1 showed a consistent correlation with the infiltration level of neutrophils and macrophages in HNSC tumors (**Figure 6A**). However, SphK1 expression showed a negative correlation with the infiltration level of B cells in the HNSC tumors, and no consistent correlation was observed with the other cell types (**Figure 6A**).

We also analyzed the differential expression of LPP3 (*PPAP2B*) across all TCGA tumors using Gene_DE module. As shown in **Figure 7**, besides HNSC, the expression of *PPAP2B* is decreased significantly in several cancer types, including the cancer of the urinary bladder, colon, esophagus, liver, pancreas, cholangiocarcinoma, lung adenocarcinoma, and lung squamous cell carcinoma.

Discussion

OSCC is the most common cancer in the Indian subcontinent, and it is one of the leading causes of cancer-related deaths among Indian men (Mallath et al. 2014). S1P signaling has been shown to play a crucial role in several processes integral to carcinogenesis, including angiogenesis, invasion, metastasis, development to resistance to chemo-radiation (Ogretmen 2018). SphK1, a key enzyme involved in S1P synthesis, promotes tumor progression, invasion, metastasis, and chemoresistance in HNSCC, and its expression level correlates with patient survival (Tamashiro et al. 2013, 2014; Kato et al. 2018). Previously, we had reported that mRNA expression of SphK1 is overexpressed in the tumors of 70% of OSCC patients. There was an overall 73% increase in the SphK1 expression in tumors than adjacent normal tissues (Vishwakarma et al. 2017). Consistent with our qRT-PCR data, we found the high expression of SphK1 by IHC in malignant epithelial cells, keratin pearl, and stromal cells of OSCC tumors. These findings were in accordance with a previously published study (Kato et al. 2018). SphK1 expression has been shown to associate with the invasiveness of OSCC tumors and the poor prognosis of patients (Kato et al. 2018).

Here, we have reported for the first time, expression of SphK2 by IHC in OSCC tumors. Low immunoreactivity seen in OSCC tumors is consistent with our qRT-PCR data, where a decrease in SphK2 mRNA expression was noted in 71% of OSCC patients (Vishwakarma et al. 2017). In multivariate linear regression analysis, tumor size was an independent negative predictor of SphK2 expression. In corroboration of our study, *SphK2*-deficient mice produced high-grade adenomas and large tumors in a mouse model of colitis-associated cancer (Liang et al. 2013). On the contrary, high expression of SphK2 has been reported in other cancer types, including breast (Antoon et al. 2011), lung (Liu et al. 2016), and colon cancer (Shi et al. 2017). Though both the isoforms of SphKs catalyze the reaction and form S1P; however, their roles differ in cellular functions (Neubauer and Pitson 2018). Initial studies conducted to characterize SphK2 functions have revealed that it can promote cell cycle arrest and apoptosis (Liu et al. 2003).

It has been suggested that depending on the intracellular localization, SphK2 can play pro-apoptotic or anti-apoptotic functions (Neubauer and Pitson 2018). Several mechanisms have been proposed to explain the pro-apoptotic functions of SphK2. Spiegel and colleagues suggested that SphK2 possesses a functional BH3 domain and may contribute to apoptosis by sequestering pro-survival Bcl-2 family proteins (Liu et al. 2003). SphK2 has also been shown to localize in mitochondria, where it directly binds with pro-apoptotic Bcl-2 family member, BAK, and induces latter's activation (Chipuk et al. 2012). Thus, low expression of SphK2 in oral squamous cells may suppress apoptosis, thereby contributing to neoplasia.

Our study found SGPP1 immunoreactivity in 89% of cases of OSCC, albeit it was low in two-third cases. Decreased expression of SGPP1 enhances cell migration and resistance to DNA damaging drugs (Le Stunff et al. 2004). Further, downregulation in SGPP1 causes ER stress-induced autophagy (Lépine et al. 2011). Thus, increased levels of SGPP1 in the OSCC tumors may protect the squamous cells against ER stress and autophagy, thereby promoting oral carcinogenesis. Moreover, loss of *SGPP1* in mice has been shown to induce keratinocyte differentiation (Allende et al. 2013). Thus, increased SGPP1 expression may cause dedifferentiation of oral epithelium and may contribute to oral carcinogenesis.

This is the first report showing the expression of LPP3 by IHC in OSCC tumor tissues. In the present study, we have demonstrated that LPP3 is strongly expressed in normal oral mucosa, whereas OSCC tumors show low (~60% cases) or loss (17% cases) of LPP3 expression. Together, we can conclude that protein expression of LPP3 is suppressed in OSCC tumors, which is in corroboration with our mRNA expression data and Oncomine data analysis published recently (Vishwakarma et al. 2017; Tang and Brindley 2020). Thus, the expression of LPP3 in OSCC is dysregulated at the transcriptional level; however, the mechanism of dysregulated expression of LPP3 in OSCC is not known. In addition to HNSCC, downregulation of LPP3 in the tumors has been shown in several cancer types including, colon, breast, lung (Leung 1998; Tang et al. 2019). LPP3 has been shown to regulate angiogenesis and embryonic development (Tang et al. 2015). In bivariate analysis, LPP3 negatively correlates with TNM staging and LVI of patients.

Further, in multivariate linear regression analysis, LPP3 expression was an independent negative predictor of TNM staging, LVI, PNE, and positive predictor of LNR. Previously, we have also reported a negative correlation between

tumor volume and expression of LPP3 (Vishwakarma et al. 2017), thus suggesting LPP3 might play an important role in tumorigenesis. Importantly, LPP3 has been shown to decrease the growth, survival, and tumorigenesis of ovarian cancer cells (Tanyi et al. 2003). LPP3 is a broad specificity plasma membrane-bound lipid phosphate phosphatase that can dephosphorylate various lipid phosphates, including phosphatidate, lysophosphatidic acid (LPA), S1P, ceramide-1-phosphate, and diacylglycerol pyrophosphate present in the extracellular milieu (Tang et al. 2015). Downregulation of LPP3 in OSCC may lead to accumulation of S1P in squamous epithelial cells, which may promote carcinogenesis by various mechanisms such as regulating cell proliferation, angiogenesis, and metastasis. Thus, LPPs may negatively regulate oral carcinogenesis. Whether downregulation of LPP3 in OSCC results in accumulation of other lipid phosphates is not known. Notably, LPA is present in saliva, has also been related to OSCC cell migration and invasiveness (Brusevold et al. 2014; Xu et al. 2019). On contrary, higher expression of LPP3 has been reported in the primary gliomas and glioblastoma cell lines (Chatterjee et al. 2011). In that study, authors showed that LPP3 promote tumor growth through beta-catenin pathway (Kohler et al. 2011). The reason for the differential effect of LPP3 in the different cancer model is not known.

Tumor-associated macrophages are broadly categorized into two types, M1-like macrophages and M2-like macrophages. M1-like macrophages are pro-inflammatory, exert antitumor effects, and are associated with a better prognosis of the patients (Kumar et al. 2019). Consistently, in our study, we found a positive correlation between LPP3 expression and the presence of B cells, Tregs, neutrophils, M1 type of macrophages, and DCs in the tumor microenvironment of HNSC tumors. We found a similar correlation between LPP3 expression and TIICs in lung adenocarcinoma (Nema et al. 2021). Furthermore, significantly higher expression of B cell-related genes and higher densities of $CD20^+$ B cells in HPV+ OSCC samples have been reported, associated with a better prognosis of the patients (Hladíková et al. 2019). S1P gradient and S1P receptor axis represent an obligatory signal for the trafficking of immune cells (Ogretmen 2017). Thus, downregulation of LPP3 in the tumors may destroy the S1P gradient in TME and affect the recruitment of TIICs in HNSC tumors. LPPs also dephosphorylate LPA; it has also been shown that LPA and autotaxin, an LPA synthesizing enzyme play a role in steady-state lymphocyte homing, but their impact on the regulation of adaptive immunity needs further understanding (Lee et al. 2020; Tang and Brindley 2020). This is an area of future investigation in the context of the expanding role of immunotherapy in head and neck cancer.

Acknowledgement

This work was funded by the Science and Engineering Research Board (SERB), Govt. of India's Scheme for Young Scientist research grant (SB/YS/LS-184/2013) and extramural research grant (EMR/2016/005009) by SERB to AK, ICMR senior research fellowship (ICMR/2019-6836) to SV and DBT Junior Research Fellowship to RP. We would like to thank Prof. David N Brindley, Univeristy of Alberta, Edmonton for the kind gift of LPP3 plasmids.

Conflict of Interest: The authors declare that they have no conflict of interest.

References:

Allende ML, Sipe LM, Tuymetova G, et al (2013) Sphingosine-1-phosphate phosphatase 1 regulates keratinocyte differentiation and epidermal homeostasis. J Biol Chem 288:18381–18391. https://doi.org/10.1074/jbc.M113.478420

Antoon J, White M, Slaughter E, et al (2011) Targeting NFκB mediated breast cancer chemoresistance through selective inhibition of sphingosine kinase-2. Cancer Biol Ther 11:678–689

Benesch M, Tang X, Venkatraman G, et al (2016) Recent advances in targeting the autotaxin-lysophosphatidate-lipid phosphate phosphatase axis in vivo. J Biomed Res 30:272–84

Bray F, Ferlay J, Soerjomataram I, et al (2018) Global cancer statistics 2018: GLOBOCAN estimates of incidence and mortality worldwide for 36 cancers in 185 countries. CA Cancer J Clin 68:394–424. https://doi.org/10.3322/caac.21492

Brindley D, Pilquil C (2009) Lipid phosphate phosphatases and signaling. J Lipid Res 50:S225-230

Brusevold I, Tveteraas I, Aasrum M, et al (2014) Role of LPAR3, PKC and EGFR in LPA-induced cell migration in oral squamous carcinoma cells. BMC Cancer 14:432

Chatterjee I, Humtsoe JO, Kohler EE, et al (2011) Lipid phosphate phosphatase-3 regulates tumor growth via β-catenin and Cyclin-D1 signaling. Mol Cancer 10:51. https://doi.org/10.1186/1476-4598-10-51

Chen SMY, Krinsky AL, Woolaver RA, et al (2020) Tumor immune microenvironment in head and neck cancers. Mol Carcinog 59:766–774. https://doi.org/10.1002/mc.23162

Chipuk JE, McStay GP, Bharti A, et al (2012) Sphingolipid metabolism cooperates with BAK and BAX to promote the mitochondrial pathway of apoptosis. Cell 148:988–1000. https://doi.org/10.1016/j.cell.2012.01.038

Hatoum D, Haddadi N, Lin Y, et al (2017) Mammalian sphingosine kinase (SphK) isoenzymes and isoform expression: challenges for SphK as an oncotarget. Oncotarget 8:36898–36929. https://doi.org/10.18632/oncotarget.16370

Hladíková K, Koucký V, Bouček J, et al (2019) Tumor-infiltrating B cells affect the progression of oropharyngeal squamous cell carcinoma via cell-to-cell interactions with CD8+ T cells. J Immunother Cancer 7:261. https://doi.org/10.1186/s40425-019-0726-6

Jain D, Dravid C, Singla A, et al (2019) Comparison of the Seventh and Eighth Editions of the American Joint Committee on Cancer pT and pN Classifications as Predictors of Survival in Patients With Oral Squamous

Cell Carcinoma. Am J Clin Pathol 151:292–301

Kato K, SHIMASAKI M, Kato T, et al (2018) Expression of Sphingosine Kinase-1 Is Associated with Invasiveness and Poor Prognosis of Oral Squamous Cell Carcinoma. Anticancer Res 38:1361–1368. https://doi.org/10.21873/anticanres.12359

Kohler EE, Sorio C, Chatterjee I, et al (2011) Lipid phosphate phosphatase-3 regulates tumor growth via β-catenin and Cyclin-D1 signaling. Mol Cancer 10:51. https://doi.org/10.1186/1476-4598-10-51

Kumar A, Saba JD (2018) Sphingosine-1-Phosphate. In: Choi S (ed) Encyclopedia of Signaling Molecules, 2nd edn. Springer International Publishing, Cham, Switzerland, pp 5128–5137

Kumar AT, Knops A, Swendseid B, et al (2019) Prognostic Significance of Tumor-Associated Macrophage Content in Head and Neck Squamous Cell Carcinoma: A Meta-Analysis. Front Oncol 9:656. https://doi.org/10.3389/fonc.2019.00656

Le Stunff H, Galve-Roperh I, Peterson C, et al (2002) Sphingosine-1-phosphate phosphohydrolase in regulation of sphingolipid metabolism and apoptosis. J Cell Biol 158:1039–1049

Le Stunff H, Mikami A, Giussani P, et al (2004) Role of sphingosine-1-phosphate phosphatase 1 in epidermal growth factor-induced chemotaxis. J Biol Chem 279:34290–7

Lee SC, Dacheux MA, Norman DD, et al (2020) Regulation of tumor immunity by lysophosphatidic acid. Cancers (Basel). 1202

Lei Y, Xie Y, Tan YS, et al (2016) Telltale tumor infiltrating lymphocytes (TIL) in oral, head & neck cancer. Oral Oncol 61:159–65. https://doi.org/10.1016/j.oraloncology.2016.08.003

Lépine S, Allegood J, Park M, et al (2011) Sphingosine-1-phosphate phosphohydrolase-1 regulates ER stress-induced autophagy. Cell Death Differ 18:350–61

Leung DW (1998) Molecular cloning of two alternatively spliced forms of human phosphatidic acid phosphatase cDNAs that are differentially expressed in normal and tumor cells. DNA Cell Biol 17:377–385. https://doi.org/10.1089/dna.1998.17.377

Li T, Fan J, Wang B, et al (2017) TIMER: A web server for comprehensive analysis of tumor-infiltrating immune cells. Cancer Res 77:e108-10. https://doi.org/10.1158/0008-5472.CAN-17-0307

Li T, Fu J, Zeng Z, et al (2020) TIMER2.0 for analysis of tumor-infiltrating immune cells. Nucleic Acids Res 48:W509–W514. https://doi.org/10.1093/nar/gkaa407

Liang J, Nagahashi M, Kim EY, et al (2013) Sphingosine-1-Phosphate Links Persistent STAT3 Activation, Chronic Intestinal Inflammation, and Development of Colitis-Associated Cancer. Cancer Cell 23:107–120. https://doi.org/10.1016/j.ccr.2012.11.013

Liu H, Toman R, Goparaju S, et al (2003) Sphingosine kinase type 2 is a putative BH3-only protein that induces apoptosis. J Biol Chem 278:40330–6

Liu W, Ning J, Li C, et al (2016) Overexpression of Sphk2 is associated with gefitinib resistance in non-small cell lung cancer. Tumor Biol 37:6331–6336. https://doi.org/10.1007/s13277-015-4480-1

Mallath MK, Taylor DG, Badwe RA, et al (2014) The growing burden of cancer in India: Epidemiology and social context. Lancet Oncol 15:e205-12. https://doi.org/10.1016/S1470-2045(14)70115-9

Nagahashi M, Abe M, Sakimura K, et al (2018) The role of sphingosine-1-phosphate in inflammation and cancer progression. Cancer Sci 109:3671–3678

Nema R, Shrivastava A, Kumar A (2021) Prognostic role of lipid phosphate phosphatases in non-smoker, lung

adenocarcinoma patients. Comput Biol Med 129:104141. https://doi.org/10.1016/j.compbiomed.2020.104141

Neubauer HA, Pham DH, Zebol JR, et al (2016) An oncogenic role for sphingosine kinase 2. Oncotarget 7:. https://doi.org/10.18632/oncotarget.11714

Neubauer HA, Pitson SM (2018) Sphingosine Kinase 2 (SPHK2). Encycl. Signal. Mol.

Ogawa C, Kihara A, Gokoh M, Igarashi Y (2003) Identification and characterization of a novel human sphingosine-1-phosphate phosphohydrolase, hSPP2. J Biol Chem 278:1268–72

Ogretmen B (2018) Sphingolipid metabolism in cancer signalling and therapy. Nat Rev Cancer 18:33–50

Ogretmen B (2017) Sphingolipid metabolism in cancer signalling and therapy. Nat Rev Cancer 18:33–50. https://doi.org/10.1038/nrc.2017.96

Shi W-N, Cui S-X, Song Z-Y, et al (2017) Overexpression of SphK2 contributes to ATRA resistance in colon cancer through rapid degradation of cytoplasmic RXRα by K48/K63-linked polyubiquitination. Oncotarget 8:39605–39617. https://doi.org/10.18632/oncotarget.17174

Simmons S, Sasaki N, Umemoto E, et al (2019) High-endothelial cell-derived s1p regulates dendritic cell localization and vascular integrity in the lymph node. Elife 8:e41239. https://doi.org/10.7554/eLife.41239

Tamashiro P, Shimizu Y, Kawamori T, et al (2013) The Impact of Sphingosine Kinase-1 in Head and Neck Cancer. Biomolecules 3:481–513. https://doi.org/10.3390/biom3030481

Tamashiro PM, Furuya H, Shimizu Y, Kawamori T (2014) Sphingosine kinase 1 mediates head & neck squamous cell carcinoma invasion through sphingosine 1-phosphate receptor 1. Cancer Cell Int 14:1–9. https://doi.org/10.1186/s12935-014-0076-x

Tang X, Benesch M, Brindley D (2015) Lipid phosphate phosphatases and their roles in mammalian physiology and pathology. J Lipid Res 56:2048–2060

Tang X, Brindley DN (2020) Lipid Phosphate Phosphatases and Cancer. Biomolecules 10:E1263

Tang X, McMullen TPW, Brindley DN (2019) Increasing the low lipid phosphate phosphatase 1 activity in breast cancer cells decreases transcription by AP-1 and expressions of matrix metalloproteinases and cyclin D1/D3. Theranostics 9:6129–6142. https://doi.org/10.7150/thno.37094

Tanyi JL, Morris AJ, Wolf JK, et al (2003) The human lipid phosphate phosphatase-3 decreases the growth, survival, and tumorigenesis of ovarian cancer cells: Validation of the lysophosphatidic acid signaling cascade as a target for therapy in ovarian cancer. Cancer Res 63:1073–1082

Vishwakarma S, Agarwal R, Goel SK, et al (2017) Altered Expression of Sphingosine-1-Phosphate Metabolizing Enzymes in Oral Cancer Correlate With Clinicopathological Attributes. Cancer Invest 35:139–141. https://doi.org/10.1080/07357907.2016.1272695

Waggoner DW, Martin A, Dewald J, et al (1995) Purification and Characterization of a Novel Plasma Membrane Phosphatidate Phosphohydrolase from Rat Liver (∗). J Biol Chem 270:19422–19429. https://doi.org/https://doi.org/10.1074/jbc.270.33.19422

Wary KK, Humtsoe JO (2005) Anti-lipid phospate phosphohydrolase-3 (LPP3) antibody inhibits bFGF- and VEGF-induced capillary morphogenesis of endothelial cells. Cell Commun Signal 3:9. https://doi.org/10.1186/1478-811X-3-9

Xu M, Yin H, Cai Y, et al (2019) Lysophosphatidic acid induces integrin β6 expression in human oral squamous cell carcinomas cells via LPAR1 coupling to Gα(i) and downstream SMAD3 and ETS-1 activation. Cell Signal 60:81–90

Figure Legends

Figure 1. Expression of SphK1 in OSCC tumors by IHC. **A-C**) neoplastic epithelium, **C**) Keratin pearl, **D**) Neural bundle, **E**), Skeletal muscle and **F**) Blood Vessels. N=Adjacent non-neoplastic mucosa. T= neoplastic mucosa

Figure 2. Expression of SphK2 in normal oral mucosa (**A-D**) and OSCC tumors (**E-H**) by IHC. **G**, Skeletal muscle, **H**) Neurovascular bundle. N=Adjacent non-neoplastic mucosa. T= neoplastic mucosa

Figure 3. Expression of SGPP1 in OSCC tumors (**A-C**) by IHC. N=Adjacent non-neoplastic mucosa. T= neoplastic mucosa

Figure 4. Expression of LPP3 in normal oral mucosa (**A-B**) and OSCC tumors (**C-F**) by IHC. N=Adjacent non-neoplastic mucosa. T= neoplastic mucosa

Figure 5. Expression of LPP3 and SphK2 decreases in the OSCC tumors. **A,** Western blotting for LPP3, SphK2, SGPP1 and actin was performed in tumor tissues (T1, T2, T3 and T4) and adjacent normal tissues (N1, N2, N3 and N4) from the same patients. **B, D and F,** Densitometric analysis was performed with Image J software and ratio of target protein/beta actin for each sample is shown with the bar diagram. **C, E and G,** Average of target protein/beta actin was calculated and values are shown as mean +/-SDEV. T-test was performed to compare the difference in mean.

Figure 6. Correlation of mRNA expression of S1P metabolizing enzymes with immune infiltration level in HNSC (N= 522), HPV negative (N=422) and HPV positive (N=98) patients was determined using Tumor Immune Estimation Resource 2.0 (TIMER 2.0). **A**. Heat map was generated for showing the positive, negative or no correlation between gene expression and infiltration level of immune cells. **B.** Representative dot plots were drafted between *PPAP2B* expression expression Log2 TPM (transcript per million) and infiltration level.

Figure 7. Distributions of *PPAP2B* gene expression levels are displayed using box plots. The statistical significance computed by differential analysis (edgeR) on RNA-Seq raw counts is annotated by the number of stars (*: p-value < 0.05; **: p-value <0.01; ***: p-value <0.001).

Figure1

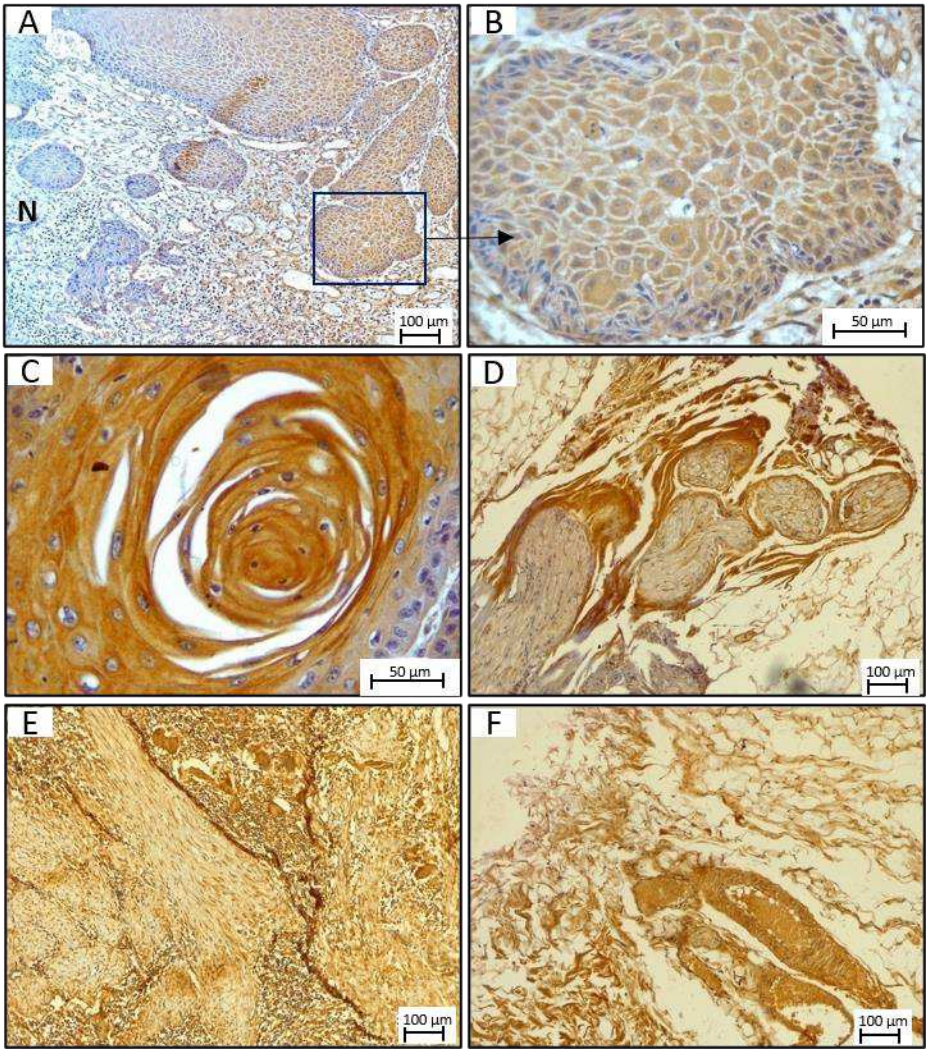

Figure 2

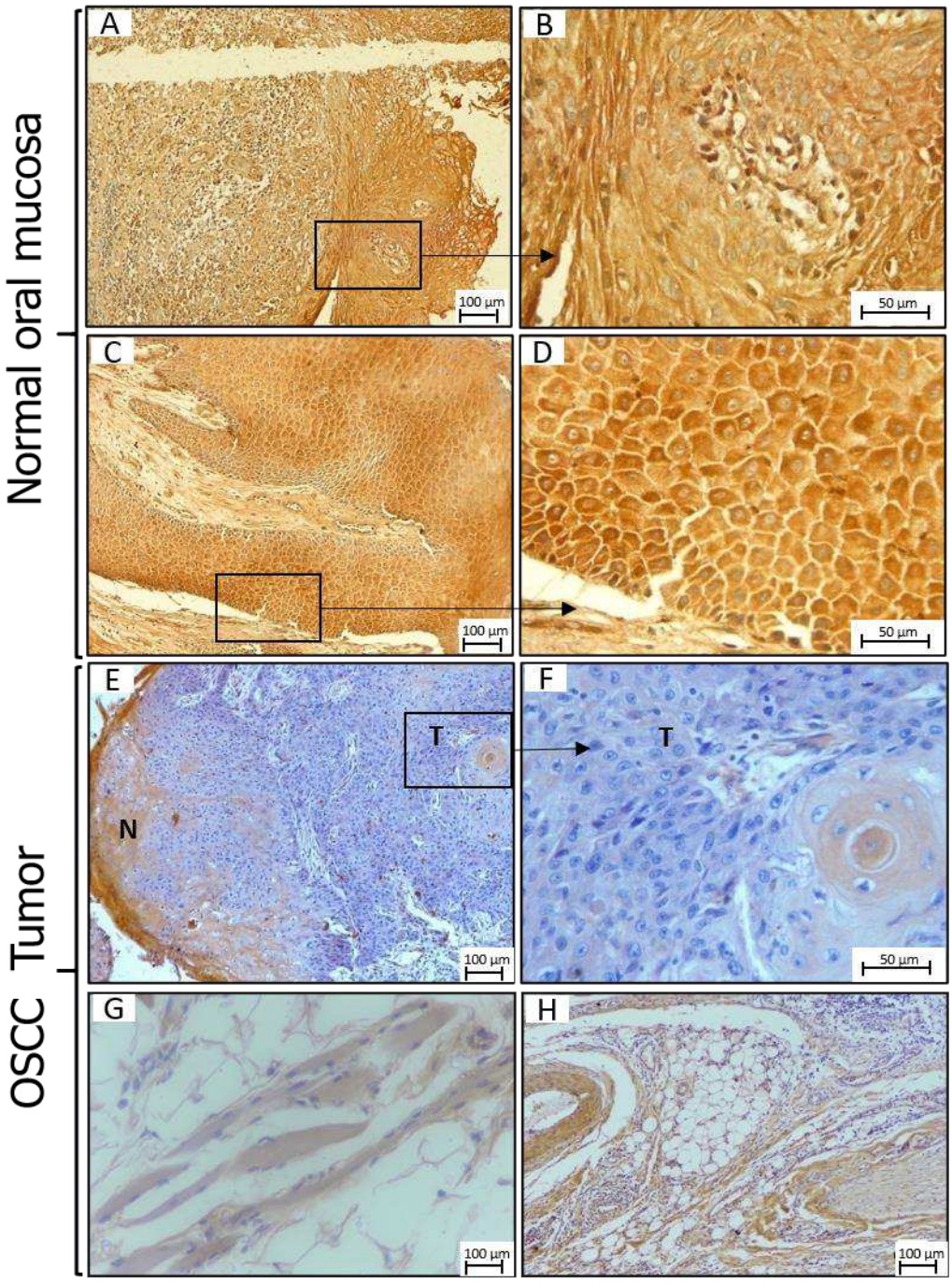

Figure 3

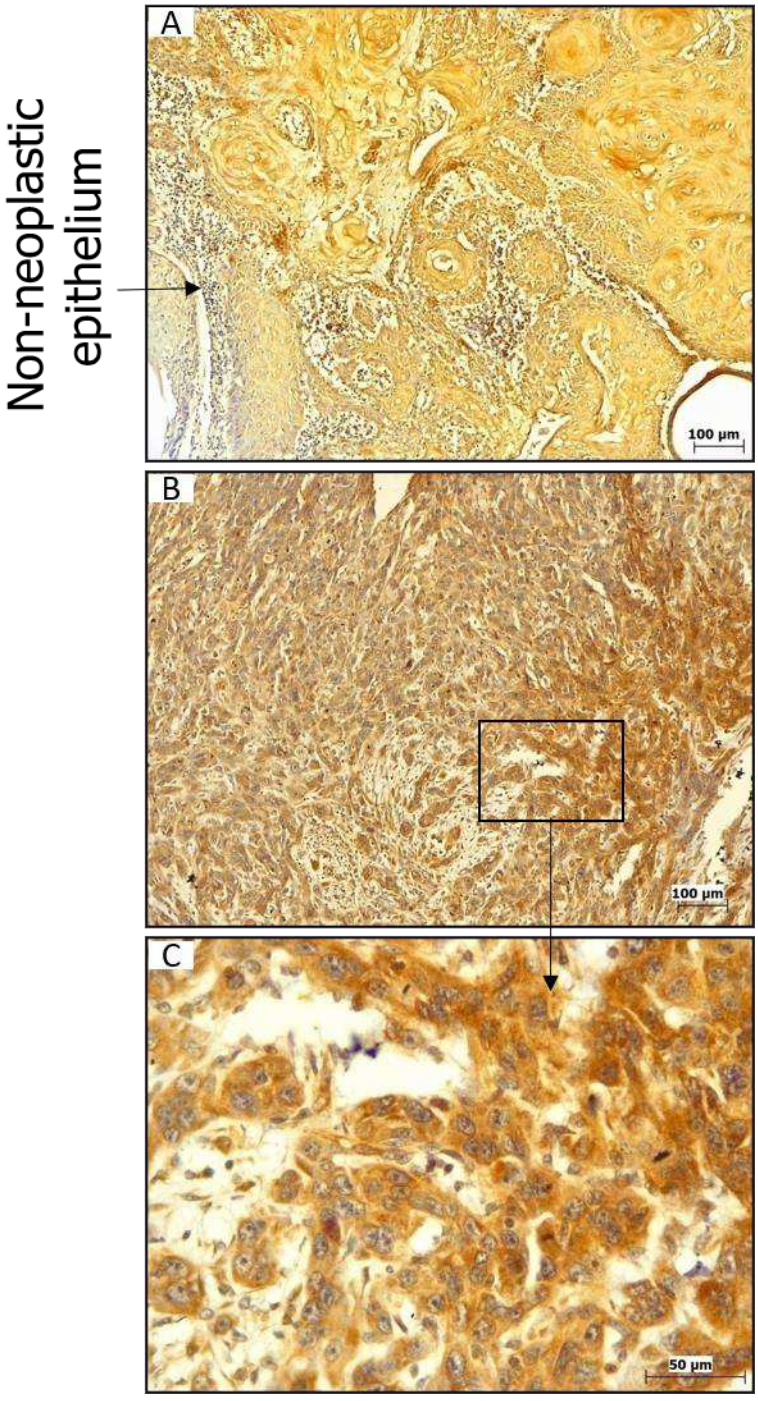

Figure 4

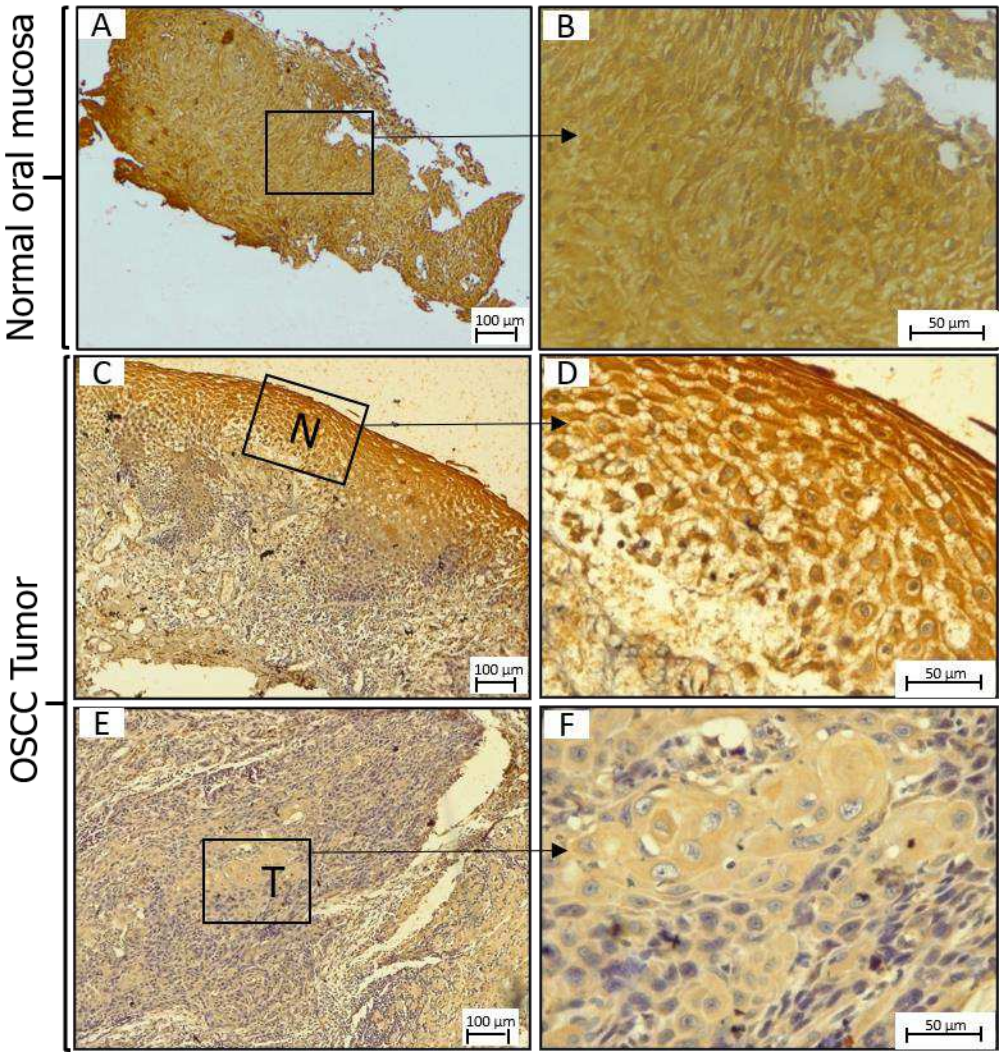
Normal oral mucosa
OSCC Tumor
A
B
C
D
E
F
N
T
100 µm
50 µm
100 µm
50 µm
100 µm
50 µm

Figure 5

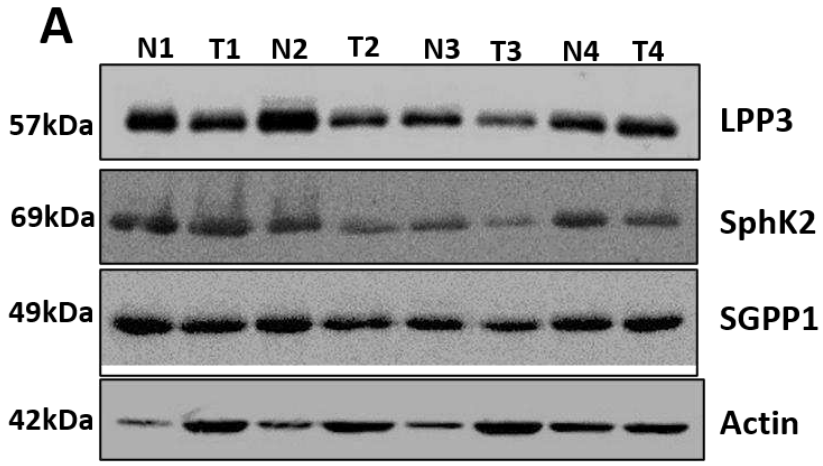
A
N1 T1 N2 T2 N3 T3 N4 T4
57kDa
LPP3
69kDa
SphK2
49kDa
SGPP1
42kDa
Actin

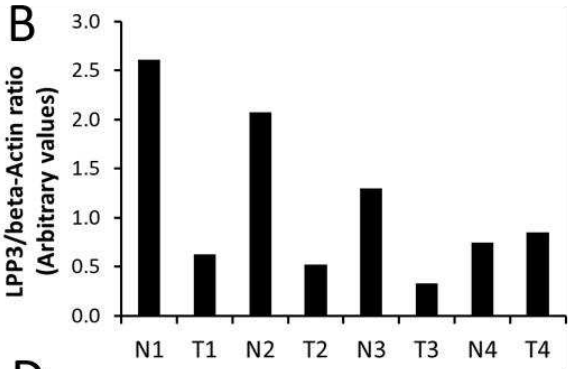
B
LPP3/beta-Actin ratio (Arbitrary values)
3.0
2.5
2.0
1.5
1.0
0.5
0.0
N1 T1 N2 T2 N3 T3 N4 T4

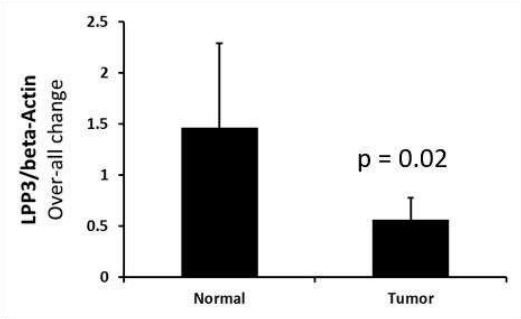
C
LPP3/beta-Actin Over-all change
2.5
2
1.5
1
0.5
0
p = 0.02
Normal
Tumor

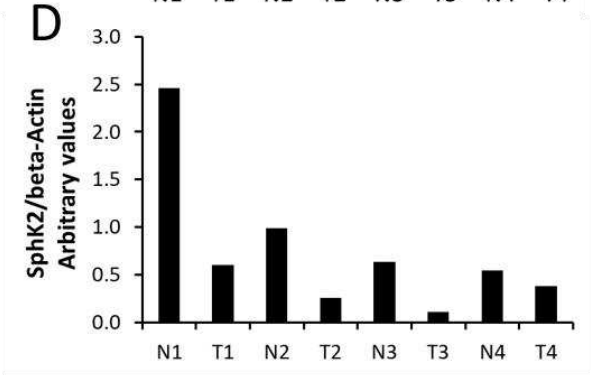
D
SphK2/beta-Actin Arbitrary values
3.0
2.5
2.0
1.5
1.0
0.5
0.0
N1 T1 N2 T2 N3 T3 N4 T4

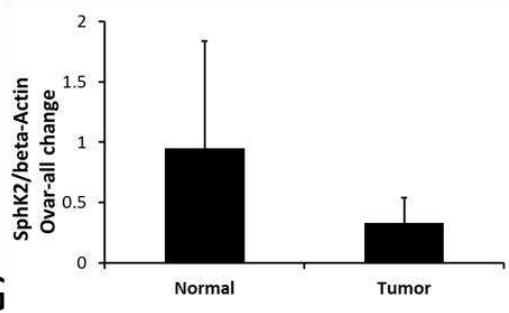
E
SphK2/beta-Actin Ovar-all change
2
1.5
1
0.5
0
Normal
Tumor

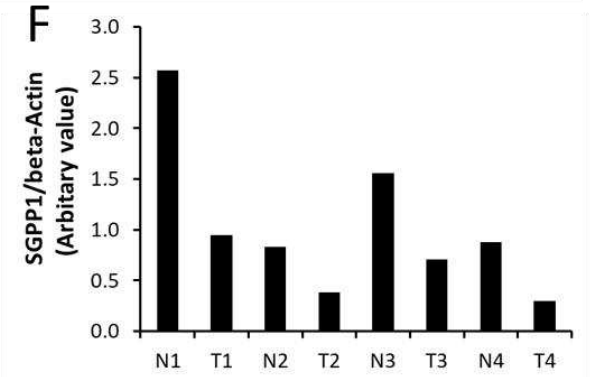
F
SGPP1/beta-Actin (Arbitrary value)
3.0
2.5
2.0
1.5
1.0
0.5
0.0
N1 T1 N2 T2 N3 T3 N4 T4

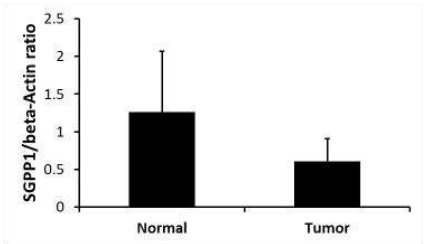
G
SGPP1/beta-Actin ratio
2.5
2
1.5
1
0.5
0
Normal
Tumor

Figure 6

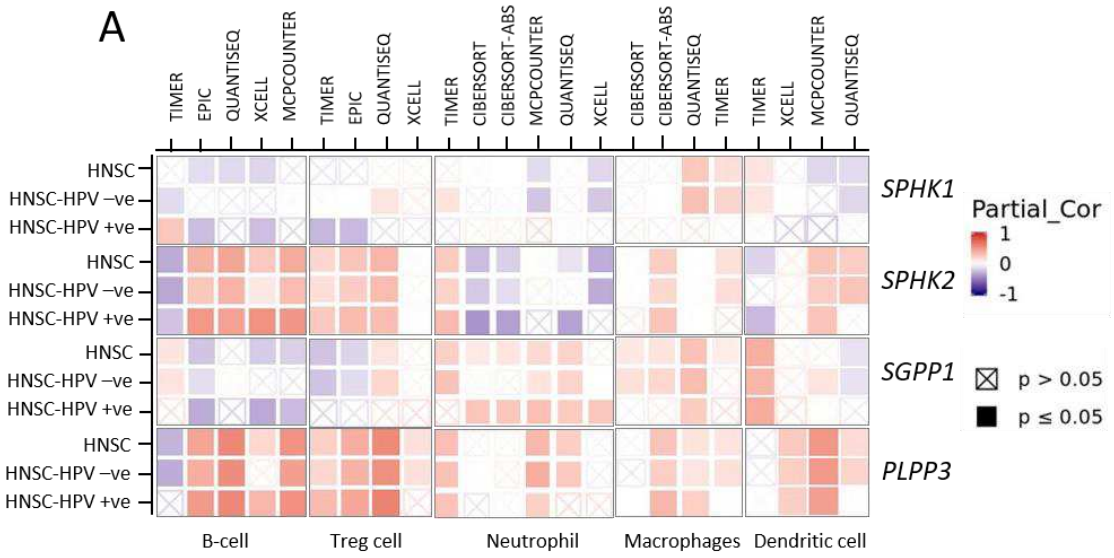
A
TIMER
EPIC
QUANTISEQ
XCELL
MCPCOUNTER
CIBERSORT
CIBERSORT-ABS
HNSC
HNSC-HPV –ve
HNSC-HPV +ve
SPHK1
SPHK2
SGPP1
PLPP3
Partial_Cor
1
0
-1
p > 0.05
p ≤ 0.05
B-cell
Treg cell
Neutrophil
Macrophages
Dendritic cell

B

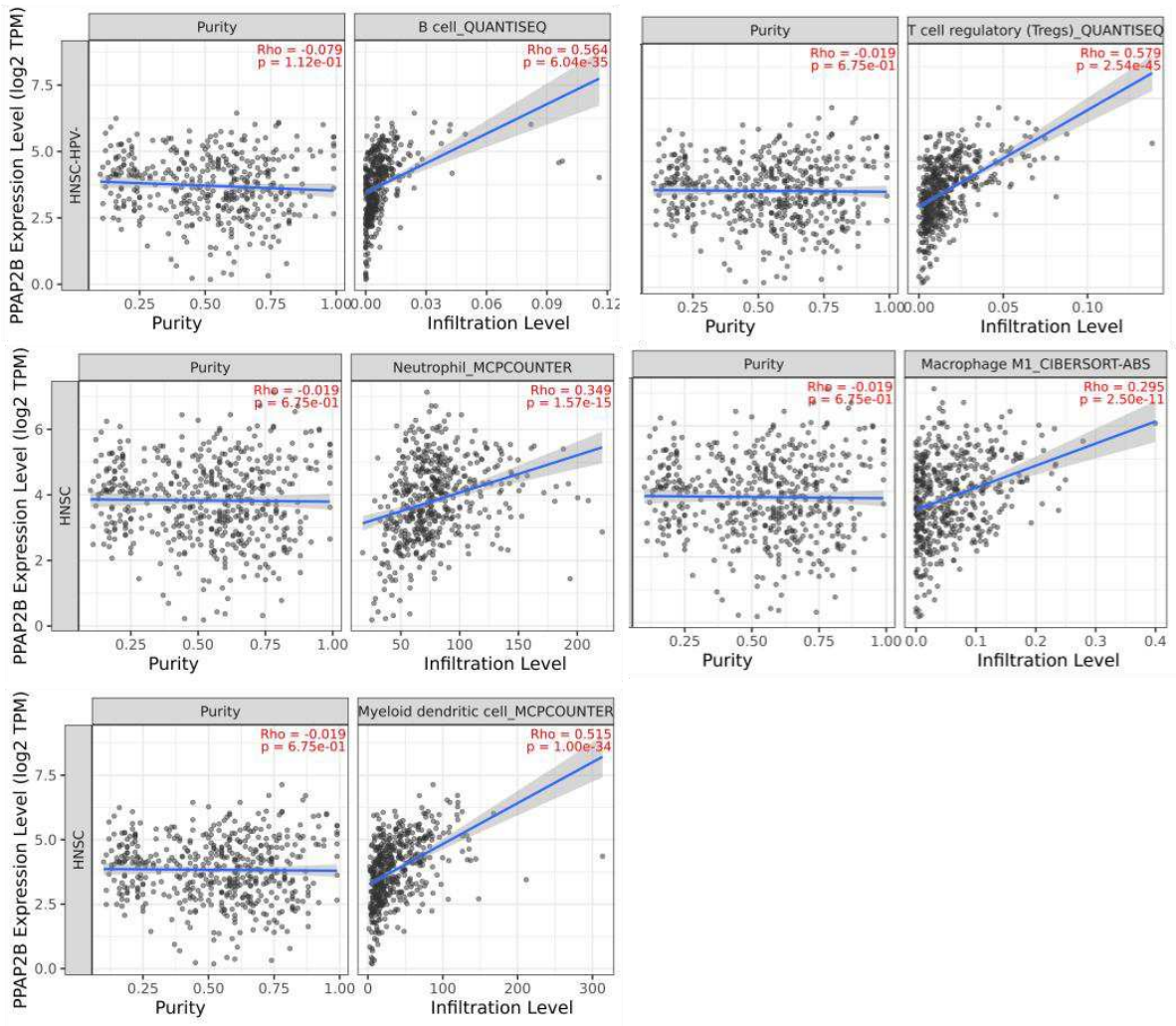
PPAP2B Expression Level (log2 TPM)
Purity
B cell_QUANTISEQ
T cell regulatory (Tregs)_QUANTISEQ
Neutrophil_MCPCOUNTER
Macrophage M1_CIBERSORT-ABS
Myeloid dendritic cell_MCPCOUNTER
Infiltration Level
HNSC-HPV-
HNSC
Rho = -0.079
p = 1.12e-01
Rho = 0.564
p = 6.04e-35
Rho = -0.019
p = 6.75e-01
Rho = 0.579
p = 2.54e-45
Rho = 0.349
p = 1.57e-15
Rho = 0.295
p = 2.50e-11
Rho = 0.515
p = 1.00e-34

Figure 7

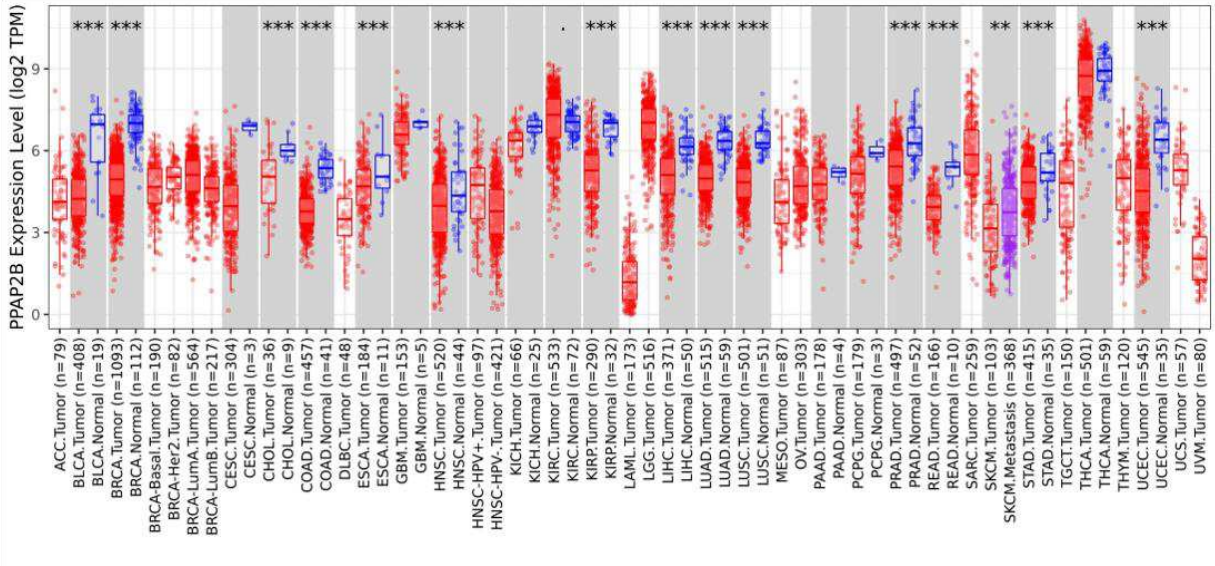
PPAP2B Expression Level (log2 TPM)
0
3
6
9
***
***
***
***
***
***
***
.
***
***
***
***
***
**
***
***
ACC.Tumor (n=79)
BLCA.Tumor (n=408)
BLCA.Normal (n=19)
BRCA.Tumor (n=1093)
BRCA.Normal (n=112)
BRCA-Basal.Tumor (n=190)
BRCA-Her2.Tumor (n=82)
BRCA-LumA.Tumor (n=564)
BRCA-LumB.Tumor (n=217)
CESC.Tumor (n=304)
CESC.Normal (n=3)
CHOL.Tumor (n=36)
CHOL.Normal (n=9)
COAD.Tumor (n=457)
COAD.Normal (n=41)
DLBC.Tumor (n=48)
ESCA.Tumor (n=184)
ESCA.Normal (n=11)
GBM.Tumor (n=153)
GBM.Normal (n=5)
HNSC.Tumor (n=520)
HNSC.Normal (n=44)
HNSC-HPV+.Tumor (n=97)
HNSC-HPV-.Tumor (n=421)
KICH.Tumor (n=66)
KICH.Normal (n=25)
KIRC.Tumor (n=533)
KIRC.Normal (n=72)
KIRP.Tumor (n=290)
KIRP.Normal (n=32)
LAML.Tumor (n=173)
LGG.Tumor (n=516)
LIHC.Tumor (n=371)
LIHC.Normal (n=50)
LUAD.Tumor (n=515)
LUAD.Normal (n=59)
LUSC.Tumor (n=501)
LUSC.Normal (n=51)
MESO.Tumor (n=87)
OV.Tumor (n=303)
PAAD.Tumor (n=178)
PAAD.Normal (n=4)
PCPG.Tumor (n=179)
PCPG.Normal (n=3)
PRAD.Tumor (n=497)
PRAD.Normal (n=52)
READ.Tumor (n=166)
READ.Normal (n=10)
SARC.Tumor (n=259)
SKCM.Tumor (n=103)
SKCM.Metastasis (n=368)
STAD.Tumor (n=415)
STAD.Normal (n=35)
TGCT.Tumor (n=150)
THCA.Tumor (n=501)
THCA.Normal (n=59)
THYM.Tumor (n=120)
UCEC.Tumor (n=545)
UCEC.Normal (n=35)
UCS.Tumor (n=57)
UVM.Tumor (n=80)

Supplementary Files

This is a list of supplementary files associated with this preprint. Click to download.

- SupplementaryInformation01.11.21.pdf